

Lateral behavior of columns with high-strength steel coiled strip confinement

Steven M. Barbachyn, Shane Oh, Lily A. Pearson, Ashley P. Thrall, Brad D. Weldon, and Yahya C. Kurama

- In this study, the behavior of columns confined by dual-phase, high-strength steel strips was compared with the behavior of a control specimen confined using deformed reinforcing bars.
- Six full-scale specimens were tested under reversed-cyclic lateral loading and a constant applied concentric axial compression load. The varied parameters of the test specimens included confinement type, layout, and reinforcement ratio.
- The experimental results provide new knowledge for confinement reinforcement with the potential to accelerate the fabrication process and improve the behavior of reinforced concrete columns subjected to seismic loads.

Ductile, high-strength (yield strength of 100 ksi [690 MPa]) coiled steel strips (**Fig. 1**) in either a hoop or spiral configuration can offer a new approach to embedded confinement for reinforced concrete structures. Potential advantages of strip confinement, as opposed to conventional deformed reinforcing bar hoops and crossties, include the following:

- increased volume of confined concrete due to the wider and thinner strip geometry
- increased effective depth (and therefore increased moment capacity) as the thinner strip enables closer placement of the extreme longitudinal reinforcing bars to the edge of the member (or, alternatively, an opportunity to reduce cross-sectional area while maintaining the same effective depth)
- increased restraint against buckling of the longitudinal reinforcing bar after concrete cover spalling due to the larger strip width

Additional fabrication benefits include rapid placement since strips can be uncoiled, bent, and tied without splices, and reduced congestion and improved concrete placement since the thin strips can have smaller bend radii. Figure 1 illustrates these potential advantages by providing a direct comparison between a conventionally confined column using Grade 100 (690 MPa) individual reinforcing bar hoops and ties and a high-strength steel-strip-confined column with an

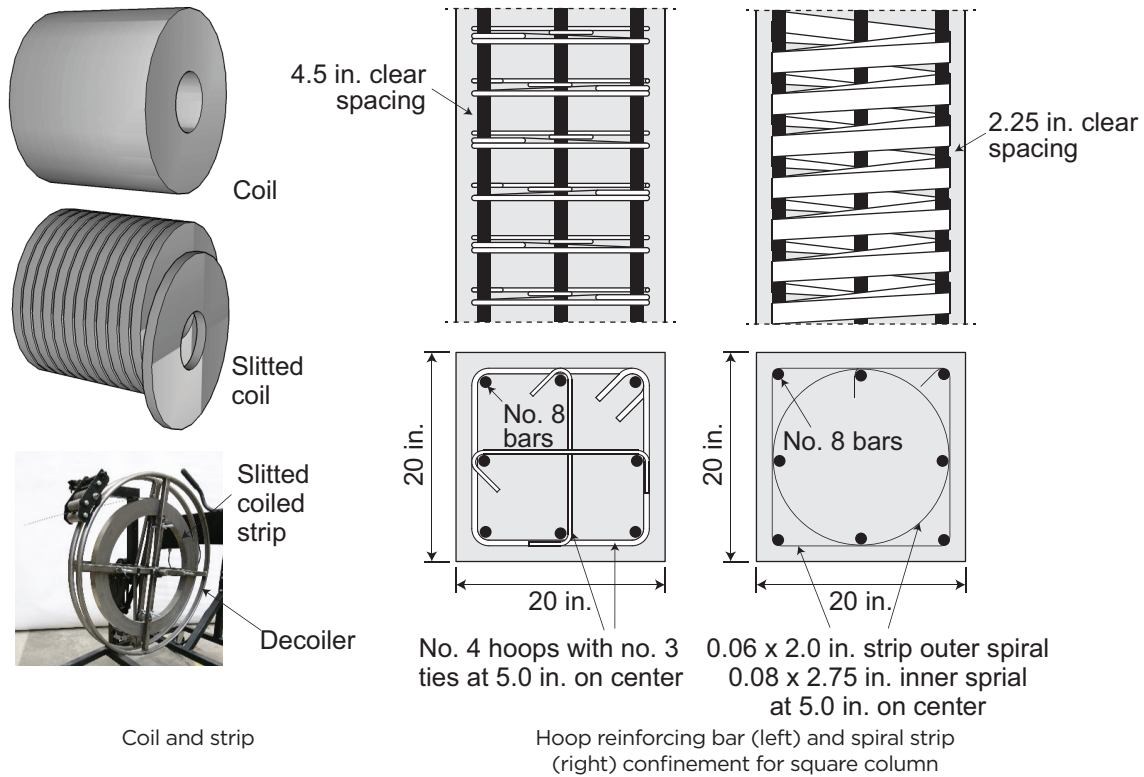


Figure 1. High-strength steel strip reinforcement. Note: No. 4 = 13M; no. 8 = 25M. 1 in. = 25.4 mm. Adapted from Barbachyn et al. (2023).

outer square perimeter strip spiral and an inner strip circular spiral. Both the conventionally confined and the strip confined column meet the specifications for columns of special moment frames in the American Concrete Institute’s *Building Code Requirements for Structural Concrete (ACI 318-19) and Commentary (ACI 318R-19)*.¹ Aside from the geometric potential of strip reinforcement, high-strength steel coil—such as the dual-phase (DP) 980/700 (yield strength of 100 ksi) used in this study—can provide increased strength as compared with ASTM A615² Grade 60 (414 MPa) deformed reinforcing steel, and increased ductility as compared with ASTM A1035³ Grade 100 deformed reinforcing steel (Fig. 2).

Given the potential benefits of this novel type of confinement reinforcement, this study experimentally investigated the lateral behavior of square reinforced concrete columns with embedded DP 980/700 strip confinement. Specifically, six full-scale specimens with 20 × 20 in. (508 × 508 mm) cross sections were tested under reversed-cyclic lateral loading and a constant applied concentric axial compression load. Varied parameters in this investigation included confinement type (strip versus reinforcing bar); confinement layout (hoops/ties, single spiral, two spirals, two spirals out of phase); and confinement reinforcement ratio.

Barbachyn et al.⁴ previously experimentally investigated the axial load behavior of square, strip-confined reinforced con-

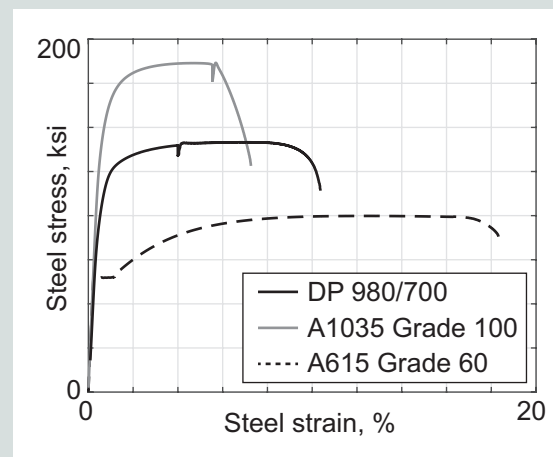


Figure 2. Comparison of stress-strain behavior for dual-phase (DP) 980/700 steel and reinforcing bar. Note: 1 ksi = 6.895 MPa. Reprinted from Barbachyn et al. (2023)

crete columns. Specifically, reduced-scale column specimens (8 × 8 in. and 10 × 10 in. [203 × 203 mm and 254 × 254 mm]) were tested under concentric axial compression until failure. Although a control (conventional) specimen confined using deformed reinforcing bar ties exhibited greater post-peak residual strength and better ductility than the strip-confined specimens, key results included the following:

- All strip-confined specimens exhibited peak strengths exceeding the nominal axial strength predicted by ACI 318-19.
- The strip-confined specimens had a similar ratio of peak axial strength to nominal axial strength as well as similar pre-peak stiffness compared with the control specimen.
- Using an outer square strip spiral and an inner circular strip spiral improved the post-peak residual strength and ductility for a cross section with eight longitudinal reinforcing bars.
- Compared with conventional reinforcing bar hoops, strip spiral or hoops can provide improved constraint to prevent corner bar buckling.

This pilot study demonstrated the viability of the strip confinement and provided valuable data (for example, findings indicating the benefits of two strip spirals) that informed the study described in the article. However, the pilot study only focused on the axial compression behavior of strip-confined columns (that is, no lateral load was applied). Therefore, to understand the behavior of strip-confined reinforced concrete columns for earthquake-resistant design, this study conducted an experimental evaluation under reversed-cyclic lateral loads and a constant applied concentric axial compression load.

Aside from the previously mentioned study, there has been no research investigating steel strip as embedded confinement reinforcement in the United States, although Robert Cummings used steel strip hoops as reinforcement as early as 1911.⁵ A few studies from other countries have been published. Shafiqat and Ali⁶ performed axial compression tests on

reinforced concrete columns confined using steel strips hoops. Also using steel strip hoop confinement, Tahir et al.⁷ performed cyclic axial load tests on reinforced concrete columns. Rizwan⁸ investigated the behavior of reinforced concrete columns confined using steel strip hoops in the hinge zone (with conventional reinforcement elsewhere) under reversed-cyclic lateral load and sustained axial load (see also Rizwan et al.⁹). There is no existing research on the lateral load behavior of reinforced concrete columns confined by steel strip spirals in the United States.

Research significance

This paper presents the measured behavior of five square reinforced concrete columns confined using DP, high-strength steel coiled strips under reversed-cyclic lateral loading combined with constant applied concentric axial compression loading, as compared with the behavior of one conventional control column with high-strength reinforcing bar confinement. This is the first research on the lateral load behavior of strip-confined reinforced concrete columns in the United States. The experimental results provide new knowledge on a novel approach for confinement reinforcement with the potential to improve the behavior of reinforced concrete columns subjected to seismic loads and to accelerate their fabrication.

Experimental investigation

Six full-scale (20 × 20 in. [508 × 508 mm] cross section) reinforced concrete columns were tested under a prescribed lateral loading protocol followed by a prescribed lateral displacement protocol, while also being subjected to a constant concentric axial compression load (Fig. 3 and Table 1). In the specimen labels, the first term denotes the confinement

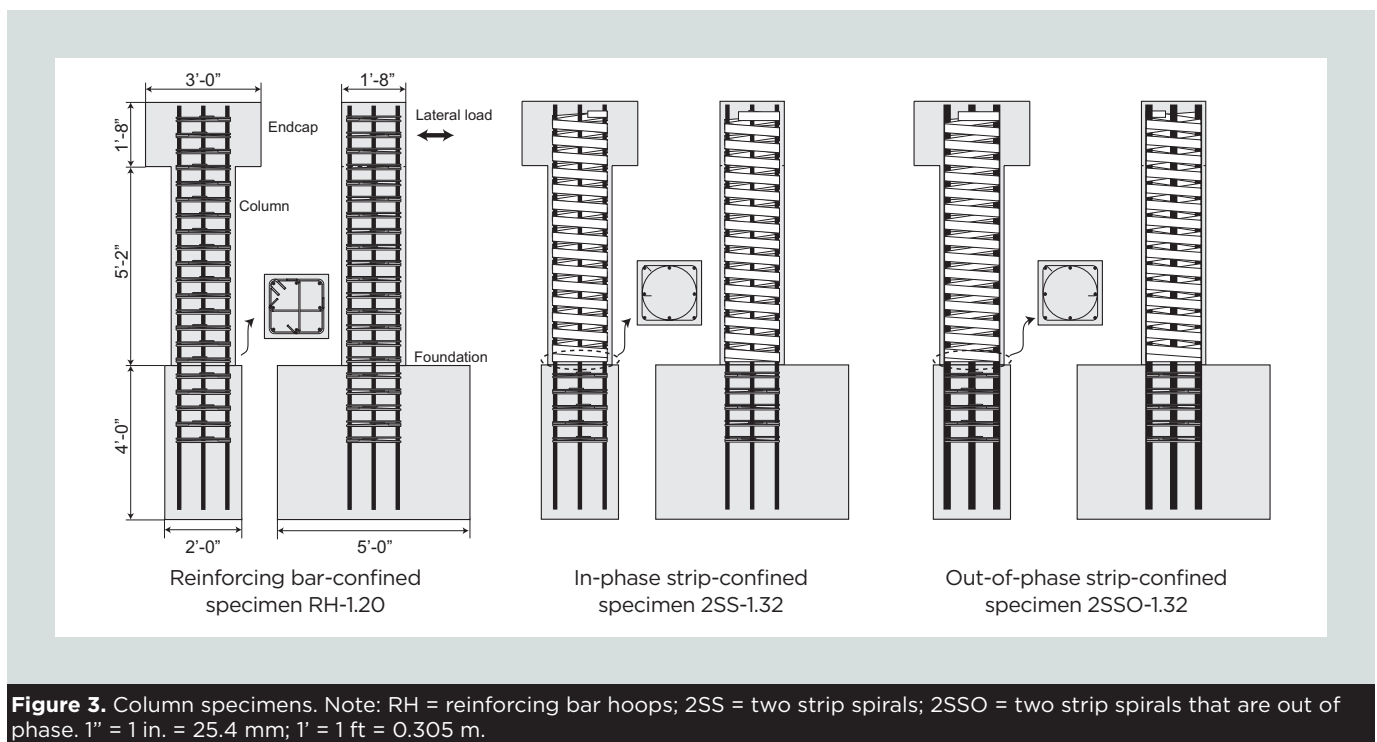


Figure 3. Column specimens. Note: RH = reinforcing bar hoops; 2SS = two strip spirals; 2SSO = two strip spirals that are out of phase. 1" = 1 in. = 25.4 mm; 1' = 1 ft = 0.305 m.

Table 1. Test specimen details

Column specimen*	f'_c , ksi	E_c , ksi	Longitudinal reinforcement				Confinement reinforcement						
			n_b	U.S. size, no.	f_{yl} , ksi	ρ_{sl} , %	Type	d_b , in.	w_s , in.	t_s , in.	s_t , in.	f_{yt} , ksi	ρ_{st} , %
Control: RH-1.20	5.73	7.11	8	8	64.9	1.58	Reinforcing bar hoops (RH) with crossties	0.50/0.38	n/a	n/a	5.00	122/133	1.20
2SS-1.32	5.69	6.89	8	8	64.9	1.58	Two strip spirals (2SS)	n/a	2.75/2.00 [†]	0.08/0.06 [†]	5.00	101/105	1.32
2SSO-1.32	5.85	5.51	8	8	64.9	1.58	Two strip spirals out-of-phase (2SSO)		2.75/2.00 [†]	0.08/0.06 [†]	5.00	101/105	1.32
SST-1.18	6.11	7.26	8	8	64.9	1.58	One strip spiral with crossties (SST)		2.75/2.00 [†]	0.08/0.06 [†]	5.00	101/105	1.18
2SS-0.98	5.91	7.43	8	8	64.9	1.58	Two strip spirals (2SS)		2.75/2.00 [†]	0.08/0.06 [†]	6.75	101/105	0.98
SS-1.15	5.84	7.29	8	8	64.9	1.58	One strip spiral (SS)		2.75	0.08	4.00	101	1.15

Note: d_b = reinforcing bar diameter; E_c = measured concrete elastic modulus on column test day (3 × 6 in. cylinders); f'_c = measured concrete compressive strength on column test day (3 × 6 in. cylinders); f_{yl} = measured longitudinal steel yield strength; f_{yt} = measured confinement steel yield strength; n/a = not applicable; n_b = number of longitudinal bars; s_t = center-to-center spacing of confinement steel; t_s = steel strip thickness; w_s = steel strip width; ρ_{sl} = longitudinal steel reinforcement ratio; ρ_{st} = volumetric reinforcement ratio of confinement steel. No. 8 = 25M. 1 in. = 25.4 mm; 1 ksi = 6.895 MPa.

* The first term denotes the confinement reinforcement type and layout and the second term denotes the confinement volumetric ratio as a percentage.

[†] Dimension for outer spiral/dimension for inner spiral.

[‡] Dimension for strip spiral/dimension for strip ties.

reinforcement type and layout, where RH = reinforcing bar hoops; SS = one strip spiral; SST = one strip spiral with crossties; 2SS = two strip spirals; and 2SSO = two strip spirals that are out of phase (Fig. 4). The second term in the specimen labels denotes the volumetric confinement reinforcement ratio as a percentage.

Specimens

The 20 × 20 in. (508 × 508 mm) specimen cross section was chosen because the dimensions are within the range of dimensions typically used in precast concrete construction (18 to 24 in. [457 to 610 mm]). The selected size of cross section allowed the application of a constant axial load of up to 15% of the gross section compression strength (with design concrete compression strength $f'_{dc} = 5$ ksi [414 MPa]). This axial load is low for building applications. However, it was the largest axial load that could be applied based on the available equipment in the laboratory.

The height of the column test specimens at the lateral load application point h_w was selected to result in the same moment-to-shear condition at the column-to-foundation interface as a full-height column in the first story of a typical

building. Considering that a realistic first-story height for a building is 12 ft (3.66 m) and that the column specimens were to be tested in a cantilever configuration, the authors chose a specimen height and lateral load application point of half the story height (that is, $h_w = 6$ ft [1.83 m]). This height corresponds to a moment-to-shear ratio of 3.6, which is within the typical range for previous column axial-flexural tests found in the literature.¹⁰

The column longitudinal (vertical) reinforcement ratio for the specimens was selected to be 1.6% based on the range of typical reinforcement ratios found in the literature (most were between 1.5% and 2.5%). This ratio also satisfies the requirements in Chapter 18 of ACI 318-19¹ for the minimum (1.0%) and maximum (6.0%) longitudinal reinforcement ratios for columns in special moment frames. The selected reinforcement ratio corresponded to eight no. 8 (25M) bars: four in the column corners and one at the centerline of each column face. The longitudinal reinforcement for all specimens had a specified yield strength $f_{syl} = 60$ ksi (414 MPa).

The parameters were as follows (Table 1 and Fig. 4):

- confinement type (strip or reinforcing bar)

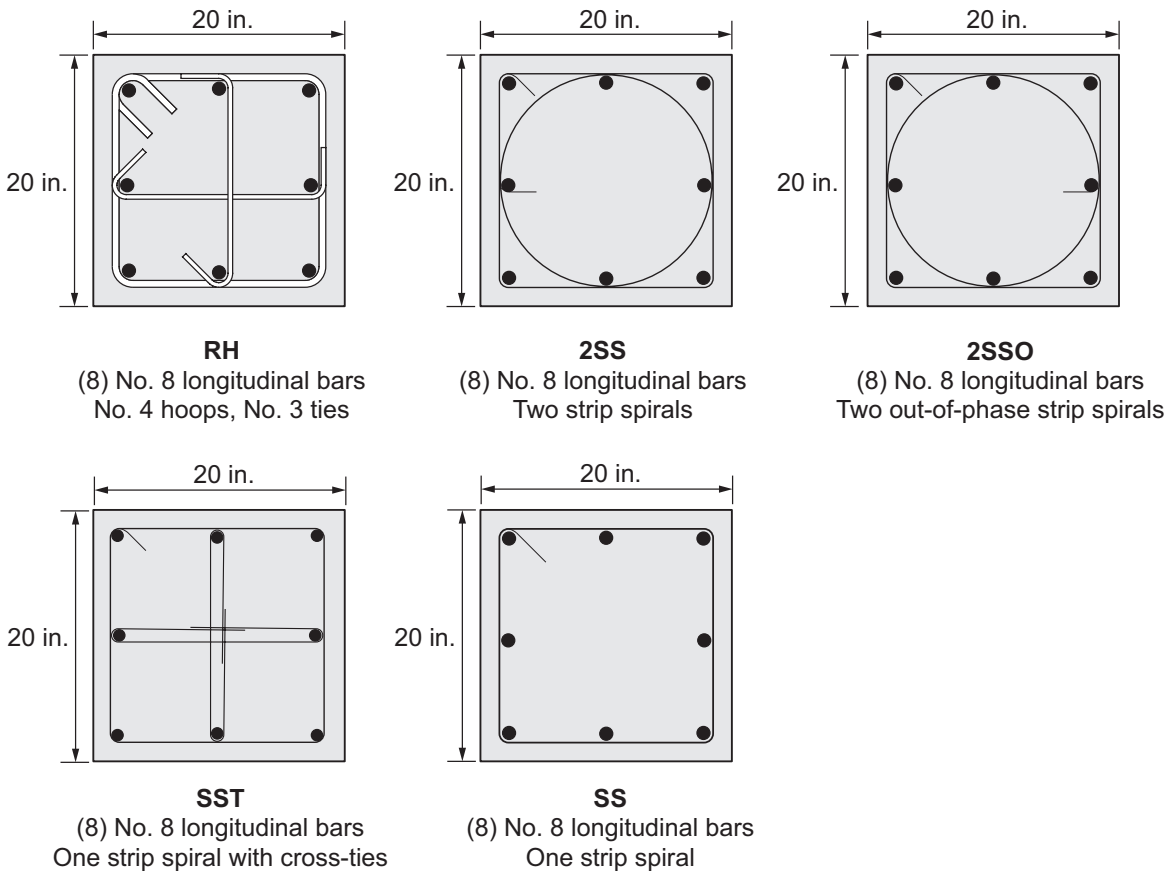


Figure 4. Column confinement layouts. Note: RH = reinforcing bar hoops; SS = one strip spiral; SST = one strip spiral with cross-tie; 2SS = two strip spirals; 2SSO = two strip spirals that are out of phase. No. 8 = 25M; 1 in. = 25.4 mm.

- confinement layout (hoops and ties, single spiral, two spirals, or two spirals out-of-phase)
- confinement reinforcement ratio

The specimens were as follows:

- Specimen RH-1.20: The control specimen—a state-of-the-practice specimen using conventional reinforcing bar cross-ties (Fig. 3). The confinement reinforcement was determined based on the requirements in Section 18.7.5 of ACI 318-19, using reinforcing bar cross-ties with a specified yield strength $f_{sy} = 100$ ksi (690 MPa) and a design concrete compression strength $f'_{dc} = 5$ ksi (34.5 MPa). The confinement layout consisted of no. 4 (13M) hoops around the column longitudinal bars with overlapping no. 3 (10M) cross-ties connecting the bars on opposite column faces (Fig. 4).
- Specimen 2SS-1.32: A strip-confined specimen with two concentric spirals (one outer square spiral around the perimeter and one inner circular spiral) and approximately the same confinement reinforcement ratio as specimen RH-1.20 (Fig. 3).

- Specimen 2SSO-1.32: A specimen identical to specimen 2SS-1.32, except that the spirals were out of phase with one another.
- Specimen SST-1.18: A strip-confined specimen with an outer strip square spiral and individual strip cross-ties connecting the longitudinal bars on opposite faces, with approximately the same confinement ratio as specimen RH-1.20.
- Specimen 2SS-0.98: A strip-confined specimen with the same layout as specimen 2SS-1.32, but a reduced confinement ratio that was achieved by increasing the center-to-center spacing of the confinement steel s_r .
- SS-1.15: A strip-confined specimen that had only one strip square spiral, with approximately the same confinement ratio as specimen RH-1.20.

For the strip-confined specimens, the strip thicknesses and widths were selected to result in strip cross-sectional areas similar to either no. 3 (10M) or no. 4 (13M) reinforcing bar, which allowed for more direct comparisons to the confinement in conventional reinforced concrete columns.

All specimens had a clear cover of 1.5 in. (38.1 mm) to the outside edges of the confined region. Because the dimension of the strip was thinner than the diameter of a conventional reinforcing bar, the effective depth of the longitudinal bars for the strip-confined specimens was slightly greater than that of a cross-section with conventional reinforcing bar.

The specimens were intended to resemble precast concrete construction as much as possible, although some simplifications were necessary for laboratory testing. The strip reinforcement did not continue into the foundation of the specimen (Fig. 3) and there was a construction cold joint between the foundation and the column specimen (discussed further in the next section). Each column was directly wet-cast against the corresponding hardened foundation with continuous longitudinal reinforcement, but the combination of the cold joint and confinement discontinuity aimed to simulate a precast concrete column base connection. In precast concrete construction, the longitudinal reinforcement would not be continuous and there would be complex connectors joining this reinforcement at the column-base connection. The specimens used continuous longitudinal reinforcement as a simplification to facilitate fabrication in a laboratory setting.

Table 2 compares each specimen to the relevant code requirements of ACI 318-19,¹ including the center-to-center spacing

of the confinement steel s_p , the clear spacing of the confinement steel s_{tc} , and the volumetric reinforcement ratio of the confinement steel ρ_{st} . Cells with a double asterisk indicate where a specimen violated a code requirement. The minimum volumetric confinement ratios were calculated in accordance with Table 18.7.5.4 of ACI 318-19, with the minimum volumetric confinement ratio for rectilinear hoops $\rho_{st,min1}$ calculated as:

$$\rho_{st,min1} = 0.60 \left(\frac{A_g}{A_{ch}} - 1 \right) \frac{f'_c}{f_{sy}} \quad (1)$$

where

A_g = gross cross-sectional area

A_{ch} = cross-sectional area of the concrete core measured to the outside edges of the confinement reinforcement

This equation was adapted from the area-based ratio in Table 18.7.5.4 of ACI 318-19 to a volumetric-based ratio for square columns with identical confinement reinforcement in both transverse directions. The minimum volumetric confinement ratio for circular spiral/hoops $\rho_{st,min2}$ was calculated as:

$$\rho_{st,min2} = 0.45 \left(\frac{A_g}{A_{ch}} - 1 \right) \frac{f'_c}{f_{sy}} \quad (2)$$

Table 2. ACI 318-19 Confinement requirements

Column specimen*	ACI 318-19 requirement					Specimen confinement reinforcement			
	$s_{t,max}$ in.†	$s_{tc,min}$ in.‡	$s_{tc,max}$ in.‡	$\rho_{st,min1}$ %§	$\rho_{st,min2}$ %¶	s_p in.	s_{tc} in.	ρ_{st} %	
RH-1.20	5.00	0.50	n/a	1.15	n/a	5.00	4.50	1.20	
2SS-1.32						5.00	2.25	1.32	
2SSO-1.32						5.00	2.25	1.32	
SST-1.18					3.00		5.00	2.25	1.18
2SS-0.98							6.75**	4.00**	0.98**
SS-1.15							4.00	1.25	1.15

Note: n/a = not applicable; s_c = center-to-center spacing of confinement steel; $s_{t,max}$ = maximum permitted center-to-center spacing of confinement steel; s_{tc} = clear spacing of confinement steel; $s_{tc,min}$ = minimum required clear spacing of confinement steel; $s_{tc,max}$ = maximum permitted clear spacing of confinement steel; ρ_{st} = volumetric reinforcement ratio of confinement steel; $\rho_{st,min1}$ = minimum volumetric reinforcement ratio of confinement steel per Equation 1; $\rho_{st,min2}$ = minimum volumetric reinforcement ratio of confinement steel per Eq. (2). 1 in. = 25.4 mm.

* The first term denotes the confinement reinforcement type and layout (RH = reinforcing bar hoops; 2SS = two strip spirals; 2SSO = two strip spirals that are out of phase; SST = one strip spiral with crossties); the second term denotes the confinement volumetric ratio as a percentage.

† From section 18.7.5.3 of ACI 318-19.

‡ From section 25.7.2.1(a) of ACI 318-19 with nominal coarse aggregate size of $\frac{3}{8}$ in.

§ From section 25.7.3.1(b) of ACI 318-19 for spirals

¶ Adapted from expression (a) in Table 18.7.5.4 of ACI 318-19 for rectilinear hoops.

** From expression (d) in Table 18.7.5.4 of ACI 318-19 for spirals and circular hoops.

*** Specimen parameters that did not meet one or more requirements of the American Concrete Institute's Building Code Requirements for Structural Concrete (ACI 318-19) and Commentary (ACI 318R-19). For minimum reinforcement ratios, $\rho_{st,min1}$ governs for spiral strips, as opposed to $\rho_{st,min2}$ as the spiral strips do not meet the strict definition of spirals in ACI 318-19.

The unique geometry of the rectilinear spiral strips does not meet the strict definitions of either rectilinear hoops or circular or spiral hoops. Therefore, both minimum reinforcement ratios are included in Table 2 as points of reference, with Eq. (1) being more applicable and conservative than Eq. (2). All specimens except specimen 2SS-0.98 met the ACI 318-19 requirements. Specimen 2SS-0.98 was intentionally designed to violate the center-to-center spacing s_p , the clear spacing s_{lc} , and the volumetric reinforcement ratio ρ_{st} requirements.

Specimen construction

The test specimens were constructed in the laboratory as follows: First, the foundation block reinforcement cage and

formwork were assembled. Next, the column cage, including strip bending for the specimens with strip spiral confinement, was fabricated. Then the column cage was integrated with the foundation block and the foundation block was cast. Finally, column formwork was assembled and the column test specimen was cast.

An arbor press was used to bend the high-strength coiled steel strip into the continuous spiral confinement for the column cages (Fig. 5). A specialized aluminum jig was designed and integrated with the arbor press to act as a press brake and control the bend radius and angle. Use of this equipment allowed for repeatability and consistency throughout the bending process. To fabricate the spiral confinement, the coiled steel strip



Figure 5. Specimen construction.

was continuously fed into the arbor press using the decoiler (Fig. 1) and bent at predetermined spacings to result in the specified out-to-out dimensions of the confined region in the column. In addition, the angle of the aluminum jig was set to create the desired pitch and spacing for the strip spiral. After the bending of the strip, a specially designed horizontal rig in the laboratory was used to assemble the column cage (Fig. 5). The two ends of the rig were constructed with plywood and functioned as templates for the placement of the column longitudinal reinforcement inside the strip confinement region. Four threaded rods were used to couple the two ends of the rig together and ensure rigid body movement as the column cage was assembled. A long center dowel rod was used to suspend the entire rig horizontally between two steel columns in the laboratory; this setup allowed the rig to rotate about its center axis. This free rotation eased the placement of the strip spiral on the rig for the final assembly of the column cage. It is envisioned that this process could be automated in the future for accelerated fabrication.

After fabrication, the bottom portion of the column cage was placed inside the assembled foundation block cage and formwork (Fig. 5). The foundation block was poured first to result in a construction cold joint at the column-to-foundation interface. Figure 5 shows three completed specimens after concrete casting and removal of the formwork (in the foreground).

Concrete properties

The target concrete compressive strength for the column specimens was $f'_{dc} = 5$ ksi (34.5 MPa). This strength was selected along with the column cross-section dimensions so that the experimental testing frame could apply the desired axial load of 15% of the gross section compressive strength.

Table 1 summarizes the measured concrete compressive strength f'_c and the measured concrete elastic modulus E_c on

the day that each column specimen was tested. For each column specimen, the concrete compressive strength was determined by testing 3×6 in. (76.2 \times 152 mm) cylinder samples (average of three) using a universal testing machine according to the procedures defined in ASTM C39.¹⁰ The nominal cylinder cross-sectional area was used to calculate the concrete stress from the measured load. The concrete elastic modulus E_c was calculated according to ASTM C469,¹¹ using the measured concrete compressive strain (via an averaging axial extensometer with a 2 in. [50.8 mm] gauge length) at a stress of 40% of the ultimate load and a stress corresponding to a strain of 50 millionths. Note that for specimen 2SSO-1.32, strain data were only available for two cylinder samples.

Steel properties

Material testing according to ASTM A370¹² was performed on the steel reinforcing bar and strip using a universal testing machine (Table 3 and Fig. 6).

Full cross-section reinforcing bar samples were tested with an 8 in. (203 mm) length between crosshead grips, with a 2 in. (50.8 mm) extensometer positioned approximately in the middle of this length. The reported bar strains up to the peak stress f_u were measured using this extensometer. Beyond the peak stress f_u , the incremental strains were approximated based on the incremental change in the distance between the crossheads. Note that the measured strains beyond the peak stress f_u are approximate (because the crosshead displacement was used) and are shown in Fig. 6 only for illustrative purposes.

The steel strip samples were machined to a dog-bone shape with a reduced width of 0.5 in. (12.7 mm) over a 3 in. (76.2 mm) length to allow the placement of the available 2 in. (50.8 mm) extensometer. Reported strip strains up to 0.04 were measured using the extensometer, with incremental

Table 3. Column reinforcement properties

Property	Confinement reinforcement				Longitudinal reinforcement
Specification	DP 980/700	DP 980/700	ASTM A1035	ASTM A1035	ASTM A615
Size	0.06 \times 2.00 in.	0.08 \times 2.75 in.	No. 3	No. 4	No. 8
f_{sy} , ksi	100	100	100	100	60
f_y , ksi	105	101	133	122	64.9
ϵ_y , %	0.640	0.660	0.650	0.650	0.270
E_s , ksi	24,000	21,900	29,300	27,500	26,100
f_u , ksi	142	137	165	157	104
ϵ_u , %	7.68	8.03	5.02	5.32	10.8
ϵ_r , %	11.5	12.5	8.08	9.56	17.8

Note: DP = dual phase. E_s = measured steel elastic modulus; f_{sy} = specified steel yield strength; f_u = measured steel peak strength; f_y = measured steel yield strength; ϵ_r = measured steel strain at rupture; ϵ_u = measured steel strain at peak strength; ϵ_y = measured steel strain at yield. No. 3 = 10M; no. 4 = 13M; no. 8 = 25M; 1 in. = 25.4 mm; 1 ksi = 6.895 MPa.

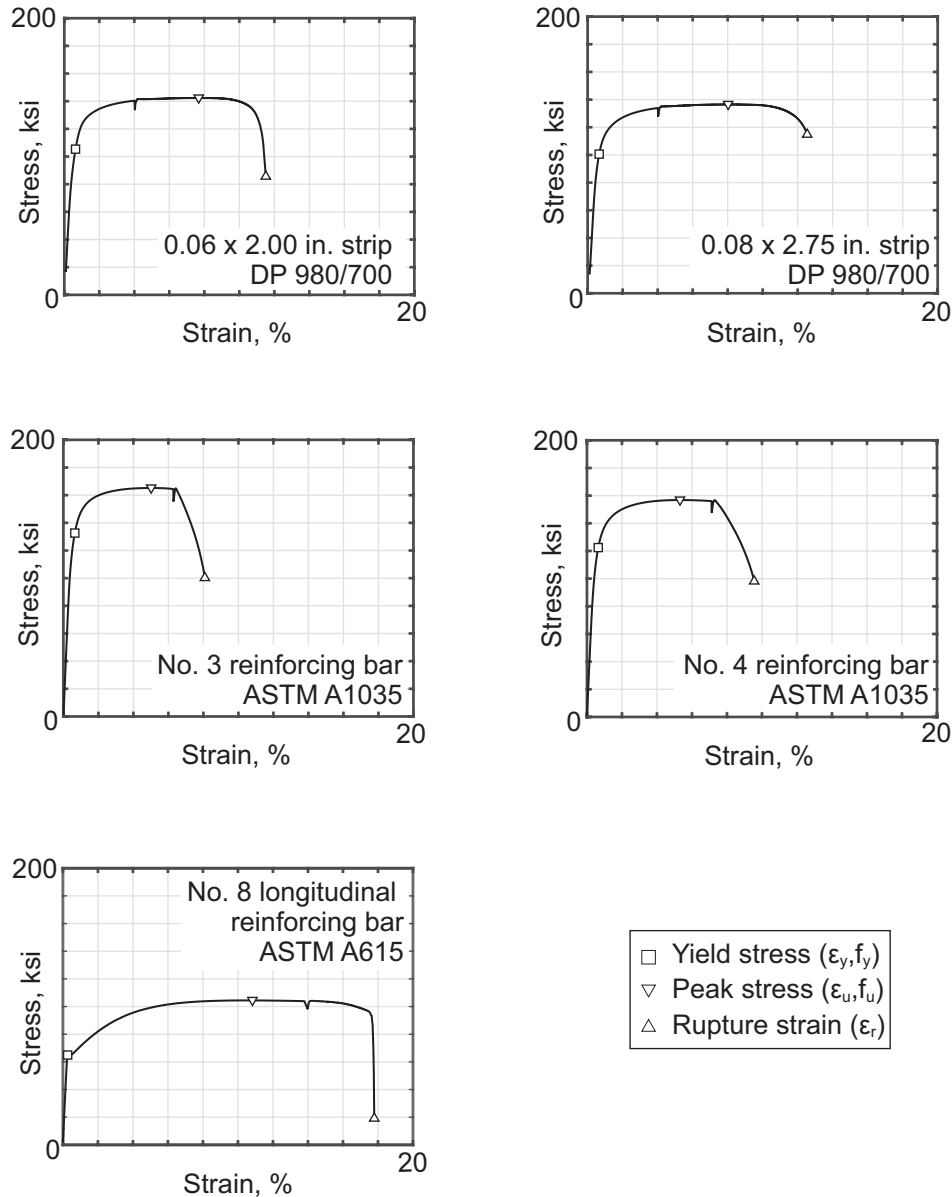


Figure 6. Strain behavior versus measure reinforcing steel stress. Note: DP = dual phase; f_u = measured peak strength; f_y = measured yield strength; ϵ_r = measured strain at rupture; ϵ_u = measured strain at peak strength; ϵ_y = measured strain at yield. No. 3 = 10M; no. 4 = 13M; no. 8 = 25M; 1" = 1 in. = 25.4 mm; 1 ksi = 6.895 MPa.

strains greater than 0.04 determined based on the incremental change in displacement of the crossheads.

Since the high-strength deformed reinforcing bar (ASTM A1035³ no. 3 and no. 4 [10M and 13M]) and the DP 980/700 strip steel did not have a yield plateau, the 0.2% offset method was used to determine the yield strength. The yield strength of the ASTM 615² no. 8 (25M) longitudinal bar was determined based on the distinctive yield plateau. A linear regression of the measured stress-strain curve was used to determine the elastic modulus for each sample in accordance with ASTM E111,¹³ at a stress range between 20 and 50 ksi (138 and 345 MPa).

Test setup and loading protocol

Figure 7 presents an elevation-view schematic, a three-dimensional rendering, and photographs of the testing setup in the laboratory. Each test specimen consisted of a foundation block tied down to the strong floor, the column test region, and an enlarged loading cap for application of the axial and lateral loads (Fig. 3 and 7).

The lateral load on each specimen was applied using a 220 kip (979 kN) capacity, servo-controlled hydraulic actuator attached to a near-rigid steel reaction frame and connected to the column at the end cap region (Fig. 7). The target loading

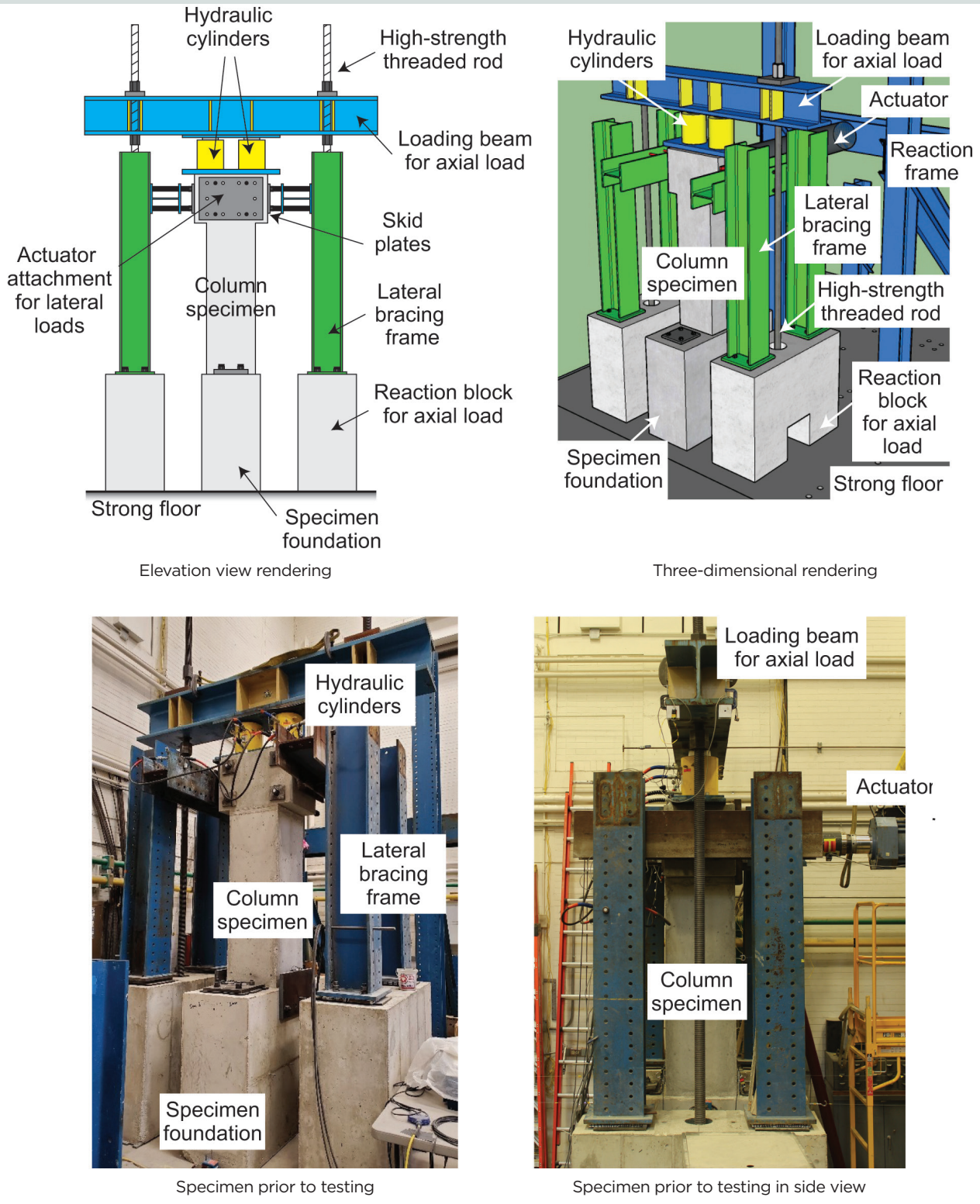


Figure 7. Test setup.

protocol was consistent with the *Acceptance Criteria for Moment Frames Based on Structural Testing* (ACI T1.1-01)¹⁴ testing protocol (Table 4). Four load-controlled series were first applied to the columns in their linear-elastic range, with three fully reversed cycles per series. Directly following the

load-controlled series, displacement-controlled series (with three fully reversed cycles per series) were conducted, with target drifts increasing by approximately 1.5 times the target drift of the prior series up to the required 3.5% validation drift prescribed by the ACI T1.1-01 acceptance criteria. Additional

Table 4. Lateral testing protocol

Series	Lateral load, kip	Column drift, %*	Column displacement, in.	Number of cycles
1	10	n.d.	n.d.	3
2	20			3
3	30			3
4	40			3
5	n.d.	0.333	0.240	3
6		0.500	0.360	3
7		0.750	0.540	3
8		1.10	0.792	3
9		1.60	1.15	3
10		2.40	1.73	3
11		3.50	2.52	3
12		4.50	3.24	3
13		5.50	3.96	3

Note: n.d. = no data. 1 in. = 25.4 mm; 1 kip = 4.448 kN.

* Column lateral displacement at line of load application divided by height from top of foundation.

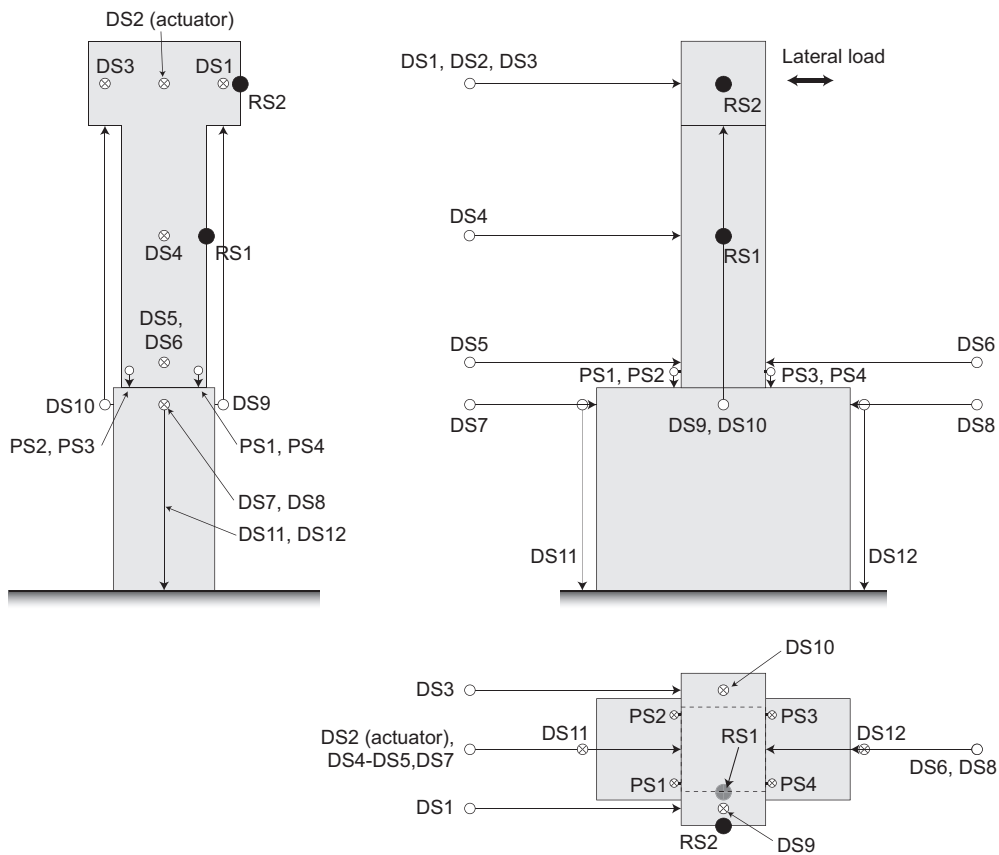


Figure 8. Instrumentation. Note: DS = string potentiometer displacement sensor; PS = spring return linear position sensor; RS = rotation sensor.

series were continued until the actuator ran out of stroke or failure of the specimen (with failure defined as the measured load dropping below 75% of the peak strength V_p in both loading directions). The same loading protocol was applied to all six specimens, except that the fourth load cycle was not implemented for specimens RH-1.20 and 2SS-1.32 because the specimens were already at the displacement limit for the first displacement control cycle. Two 250 ton (227 tonne) hydraulic jacks on top of the specimen simultaneously applied the constant concentric axial load by reacting against a steel loading beam. The magnitude of the applied load was 15% of the gross section compression strength, with this value based on the test-day concrete compressive strength. The applied load ranged from 340 to 365 kip (1510 to 1620 kN). The vertical axial force from the hydraulic jacks was resisted by high-strength, 2.5 in. (63.5 mm) diameter rods at each end of the loading beam. These threaded rods were anchored through two reinforced concrete reaction blocks that were tied down to the laboratory strong floor. In a pocket under each reaction block, there was a steel rocker plate, which allowed the rods to rotate as the column was laterally displaced. An external lateral bracing frame was used to restrain any out-of-plane movement (that is, left-right movement in Fig. 7) of the column specimen during loading.

The behavior of each test specimen was monitored using a suite of sensors (Fig. 8). To measure displacements, a combination of spring return linear position sensors and string potentiometer displacement sensors were used. Rotations were

measured using clinometers. The lateral load was measured using a load cell (internal to the actuator), and the axial load was measured using pressure transducers. The axial load jack pressure was held within 2% of the target load during each test so as to maintain a near-contact axial load as each column was displaced laterally.

Experimental results and discussion

Table 5 provides the initial stiffness K_i (measured as the average secant stiffness to the peak points of the three cycles of the series corresponding to 75% of the peak lateral load V_p for each specimen); the lateral load at initial column cracking V_c ; the peak lateral load V_p ; the lateral load at the validation-level drift (that is, drift $\Delta = 3.5\%$) V_v ; and the drift at peak lateral load Δ_p . Figure 9 shows the displacement (and drift) behavior versus lateral load for each specimen, and Fig. 10 shows the envelope of this behavior. Rocking and slip of the foundation were removed from the measurements. Figure 11 shows the axial deformation versus displacement (and drift) behavior for each specimen.

For all specimens except specimen SS-1.15, failure (lateral load less than 75% of the peak lateral load V_p in each loading direction) could not be achieved because the actuator ran out of stroke. It is expected that specimen SS-1.15 would be the most likely specimen to fail because it was confined by only a single strip spiral, meaning that the middle bars had little restraint from buckling. Although specimen SS-1.15

Table 5. Experimental results

Measured property		Specimen*					
		RH-1.20	2SS-1.32	2SSO-1.32	SST-1.18	2SS-0.98	SS-1.15
Positive loading	K_i , kip/in.	97.7	146	149	161	152	150
	V_c , kip	35.0	34.1	39.2	34.1	37.4	36.0
	V_p , kip	83.6	83.7	84.7	84.0	84.8	83.3
	V_v , kip	73.7	77.1	75.2	78.2	77.2	70.2
	V_v/V_p	0.882	0.921	0.888	0.931	0.910	0.843
	Δ_p , %	2.45	1.59	1.36	2.20	1.35	1.34
Negative loading	K_i , kip/in.	112	131	140	130	138	129
	V_c , kip	-29.5	-31.9	-32.2	-27.7	-31.8	-28.3
	V_p , kip	-88.8	-86.7	-82.1	-82.7	-84.0	-85.3
	V_v , kip	-81.7	-80.9	-75.6	-76.2	-79.5	-76.9
	V_v/V_p	0.920	0.933	0.921	0.921	0.946	0.902
	Δ_p , %	-1.93	-1.52	-1.40	-3.44	-3.44	-1.57

Note: K_i = initial stiffness; V_c = lateral load at initial column cracking; V_p = peak lateral load; V_v = lateral load at validation-level drift (that is, drift $\Delta = 3.5\%$); Δ_p = drift at peak lateral load. 1 kip = 4.448 kN; 1 kip/in. = 0.11298 kN/m.

*The first term denotes the confinement reinforcement type and layout (RH = reinforcing bar hoops; SS = one strip spiral; SST = one strip spiral with cross-ties; 2SS = two strip spirals; 2SSO = two strip spirals that are out of phase); the second term denotes the confinement volumetric ratio as a percentage.

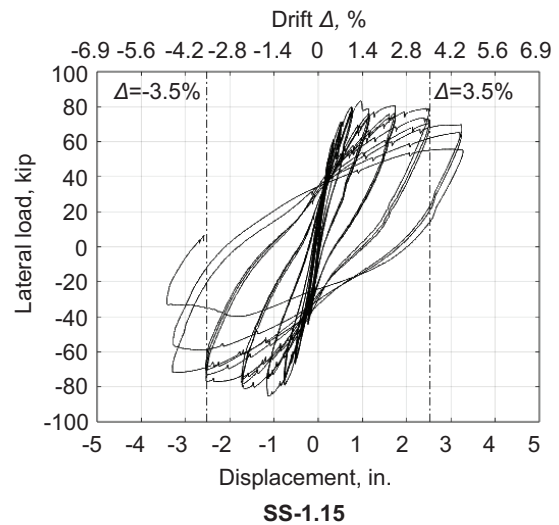
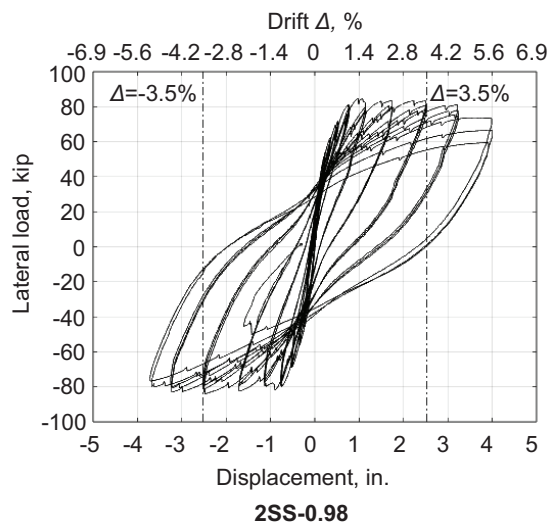
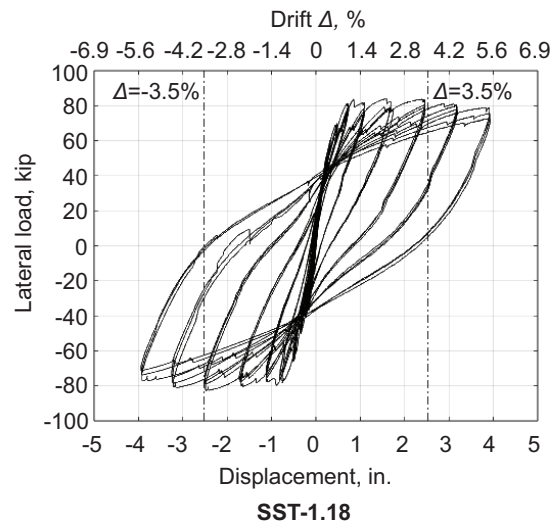
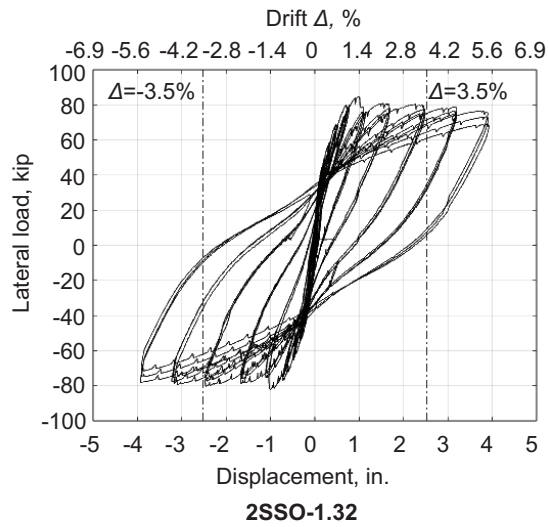
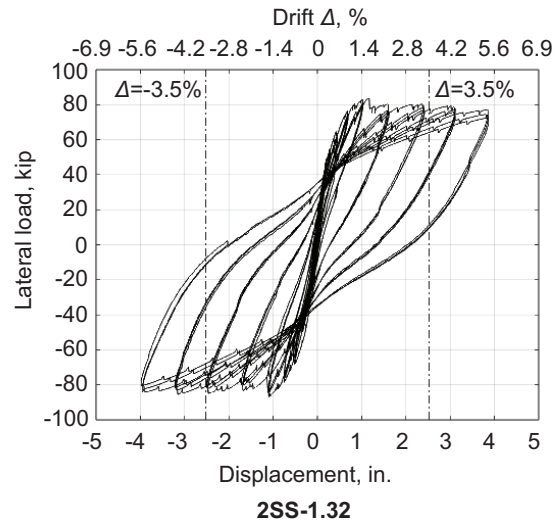
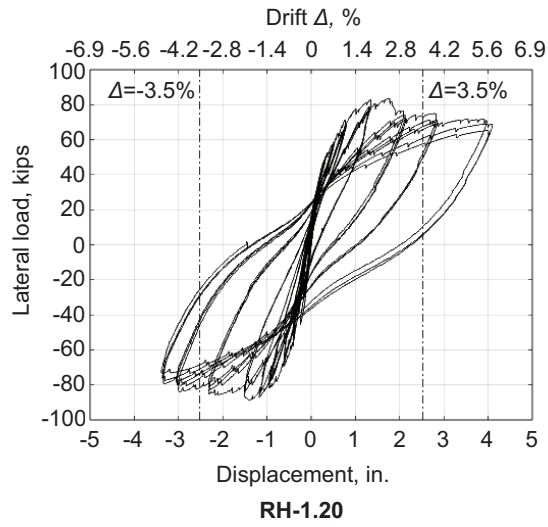


Figure 9. Displacement and drift versus lateral load. Note: RH = reinforcing bar hoops; SS = one strip spiral; SST = one strip spiral with cross-tie; 2SS = two strip spirals; 2SSO = two strip spirals that are out of phase. 1 in. = 25.4 mm; 1 kip = 4.448 kN.

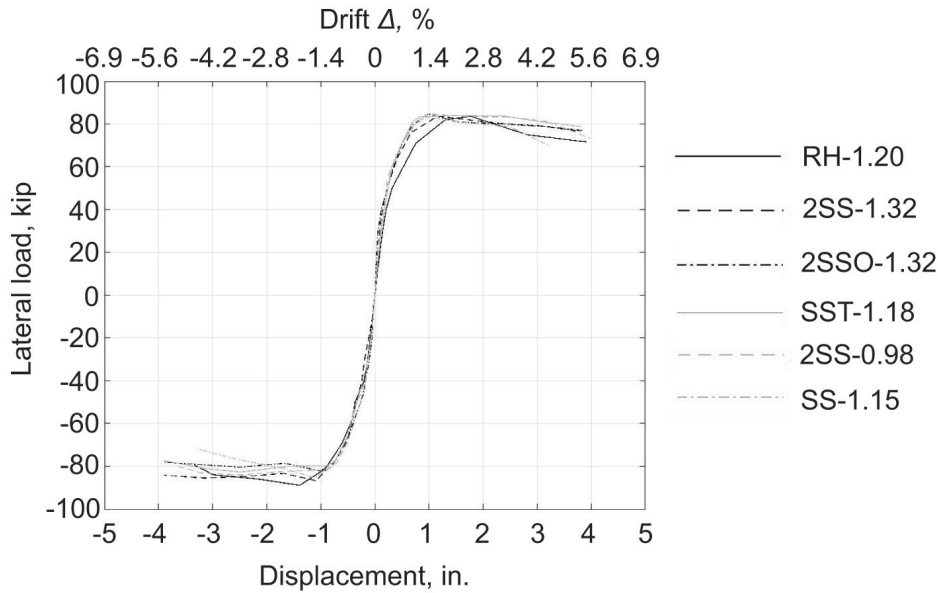


Figure 10. Displacement and drift versus lateral load for each specimen. Note: RH = reinforcing bar hoops; SS = one strip spiral; SST = one strip spiral with crosstie; 2SS = two strip spirals; 2SSO = two strip spirals that are out of phase. 1 in. = 25.4 mm; 1 kip = 4.448 kN.

met the required confinement ratio and confinement spacing of ACI 318-19,¹ the middle bars exceeded 6 in. (152 mm) clear spacing and would require lateral support in accordance with ACI 318-19. Barbachyn et al.⁴ found that in an eight bar layout, the middle bars were not adequately restrained against buckling and thus recommended the use of two strip spirals to provide restraint to these middle bars. Specimen 2SS-0.98—which had the smallest confinement reinforcement ratio and violated the ACI 318-19 requirements for center-to-center spacing s_p , clear spacing s_{ic} , and volumetric confinement reinforcement ratio ρ_{st} (Table 2)—had a load drop of 29.8% in the positive direction of the third cycle of the last series, but the third cycle in the negative direction could be not completed.

The strip-confined specimens exhibited similar peak strengths as the control specimen; their peak strengths ranged between -0.36% and $+1.43\%$ of the control column strength in the positive loading direction and between -7.54% and -2.36% in the negative loading direction. **Table 6** compares the peak lateral strengths V_p for the specimens with their nominal lateral strengths calculated using specified material properties E_n and with their nominal lateral strengths calculated using measured material properties E_{pr} . All specimens had a peak lateral strength that exceeded both of the nominal lateral strengths. For the control specimen, the ratio of the peak lateral strength to the nominal lateral strength calculated using measured material properties (V_p/E_{pr}) was 1.09 in the positive loading direction and 1.16 in the negative loading direction. In comparison, the average ratio for the strip-confined specimens was 1.06 in both the positive and negative directions. Varying the strip confinement layout (single spiral, single spiral with ties, two spirals, two spirals out-of-phase) and the confinement

reinforcement ratio had negligible impact on the peak lateral strength. Overall, the peak strength of the strip-confined specimens was comparable to that of a reinforcing-bar-confined control specimen and exceeded analytical predictions for lateral strength, even for specimen 2SS-0.98 (which violated the ACI 318-19 minimum reinforcement $\rho_{st,min1}$ requirement, as well as the center-to-center spacing and clear spacing requirements for confinement steel).

Table 6. Lateral load comparison

Column specimen*	V_p , kip	E_n , kip	E_{pr} , kip	V_p/E_{pr}
RH-1.20	+83.6/-88.8	70.8	76.5	1.09/-1.16
2SS-1.32	+83.7/-86.7	72.7	78.2	1.07/-1.11
2SSO-1.32	+84.7/-82.1		79.3	1.06/-1.04
SST-1.18	+84.0/-82.7		81.0	1.04/-1.02
2SS-0.98	+84.8/-84.0		79.7	1.06/-1.05
SS-1.15	+83.3/-85.3		79.2	1.05/-1.08

Note: E_n = nominal lateral resistance calculated using specified material properties; E_{pr} = nominal lateral resistance calculated using measured material properties; V_p = measured peak lateral load (for the positive and negative loading directions). 1 kip = 4.448 kN.

* The first term denotes the confinement reinforcement type and layout (RH = reinforcing bar hoops; SS = one strip spiral; SST = one strip spiral with crossties; 2SS = two strip spirals; 2SSO = two strip spirals that are out of phase); the second term denotes the confinement volumetric ratio as a percentage.

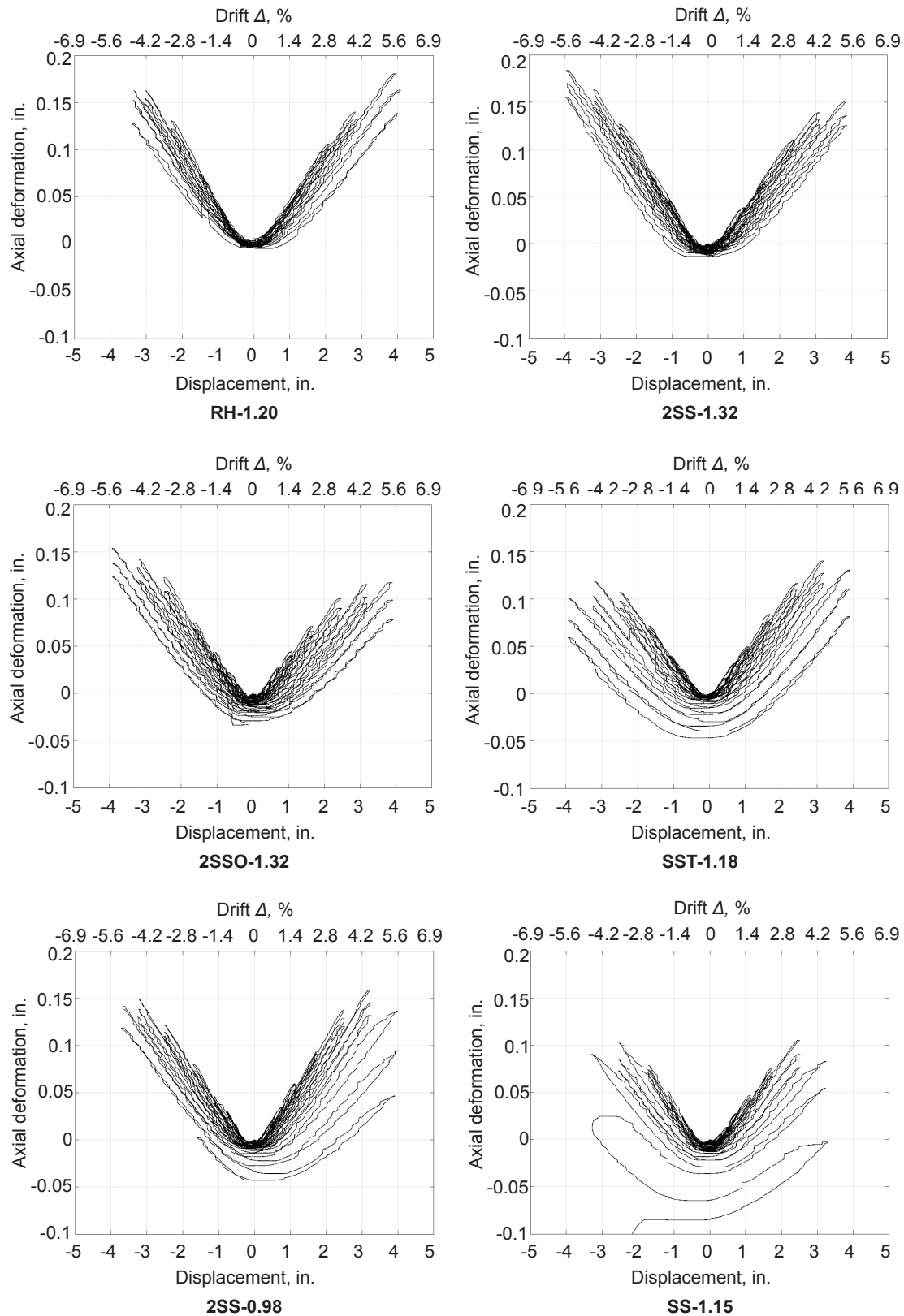


Figure 11. Displacement and drift versus axial deformation for each specimen. Note: RH = reinforcing bar hoops; SS = one strip spiral; SST = one strip spiral with crosstie; 2SS = two strip spirals; 2SSO = two strip spirals that are out of phase. 1 in. = 25.4 mm; 1 kip = 4.448 kN.

The initial stiffness K_i of all of the strip-confined specimens exceeded that of the control specimen in both loading directions (Table 5). The difference was more pronounced in the positive loading direction, where the average stiffness of the strip-confined specimens was 152 kip/in. (17,100 kN/mm), which was 55.2% higher than the stiffness of the reinforcing-bar-confined control specimen (97.7 kip/in. [11,000 kN/mm]). In the negative loading direction, the average stiffness of the strip-confined specimens was 19.3% greater than the reinforcing-bar-confined specimen. However, only one reinforcing-bar-confined specimen was tested, and additional research is needed to further investigate any impact of strip confinement on stiffness. For all of the strip-confined specimens, the stiffness in the negative loading direction was less than that in the positive loading direction. The difference in stiffness between the positive and negative directions was greatest in the specimens that had a single spiral; specifically, the stiffness was 19.3% lower in the negative direction than in the positive direction in specimen SST-1.18, and the difference between the positive and negative directions was 14.0% in specimen SS-1.15. In contrast, specimen 2SSO-1.32, with two out-of-phase spirals, had the least decrease in stiffness from the positive to the negative direction (6.04%). As a point of comparison, specimen RH-1.20 had a 14.6% increase in stiffness from the positive to the negative direction. These findings suggest that there may be some directionality associated with the orientation of the spiral and the loading direction; also, two out-of-phase spirals may provide the most consistent stiffness because they form an almost x-braced system of restraint (Fig. 3). This is an area for future research. The lateral load at initial column cracking V_c was similar among all of the tested specimens (Table 5).

Importantly, all specimens met the ACI T1.1-01¹⁴ criterion that the lateral load at the third complete cycle for the validation drift ratio of 3.5% was not below 75% of the peak load

(Table 5). This finding indicates that strip confinement has the potential to provide the necessary strength and ductility for high seismic regions.

The lateral load versus displacement (and drift) behavior of the specimens (Fig. 9 and 10) indicates that the effect of the loss of cover at the peak load on lateral behavior was greater for the reinforcing-bar-confined specimen than for the strip-confined specimens. This finding supports the expected benefit from the larger confined core area in strip-confined columns, where the strip forms an almost tubelike reinforcement. Table 5 compares the lateral load at validation-level drift to the peak load V_v/V_p ; it shows that the values were generally greater for the strip-confined specimens than for the control specimen, a finding that further indicates that residual strength behavior is improved by using strip confinement.

The axial deformation behavior of specimen 2SS-1.32 was very similar to that of the reinforcing-bar-confined control specimen RH-1.20 (Fig. 11). Note that positive deformations correspond to axial lengthening and negative deformations correspond to shortening. Among the other strip-confined specimens, there was notable residual shortening in specimens 2SSO-1.32, 2SS-0.98, and SS-1.5. Each of these specimens also exhibited significant longitudinal bar buckling at the base (as observed in the excavated specimens after testing). This is discussed further in the next paragraph. Specimen SST-1.18 also exhibited notable residual shortening, but not noticeable longitudinal bar buckling. This finding may indicate that the using two strip spirals offers better axial performance than using one spiral and ties.

After testing was completed, the specimens were excavated at their base to better understand any longitudinal bar buckling or confinement steel rupture (Fig. 12). While the tubelike reinforcement formed by the steel strip provides benefits in



Figure 12. Photographs of excavated specimens after testing. Positive and negative labels indicate the compression face under that loading direction. Note: RH = reinforcing bar hoops; SS = one strip spiral; SST = one strip spiral with crosstie; 2SS = two strip spirals; 2SSO = two strip spirals that are out of phase.

terms of core confinement, it also forms a smooth surface with the concrete, which means it could potentially contribute to more cover spalling under the cyclically applied load. Figure 12 shows that the area of concrete excavated for the strip-confined specimens was much greater than that for the control specimen. This visible difference reflects that it was relatively easier to remove the spalled concrete for the strip-confined specimens. In control specimen RH-1.20, there was no visible buckling of the longitudinal bars. In specimen 2SS-1.32, which was the most similar to the control specimen, there was also no visible buckling of the longitudinal bars. This finding indicates that the two strip spirals can provide a similar restraint to bar buckling as the conventional deformed reinforcing bar hoops and ties. Note that specimen 2SS-1.32 had a slightly larger volume of confinement reinforcement than specimen RH-1.20 due to the confinement geometry for the two-strip spiral layout (that is, one inner circular spiral and one outer square spiral). In specimen 2SSO-1.32, which had the same volume of strip spiral reinforcement as specimen 2SS-1.32 but had out-of-phase inner and outer spirals, there was significant corner bar buckling on the positive loading side of the specimen. In the out-of-phase specimen, the corners would be less effectively confined because the outer and inner spirals would coincide at only discrete locations, as opposed to continuously coinciding (Fig. 3). Thus, the out-of-phase spirals may reduce the restraint from buckling at the corners. Specimen SST-1.18, which featured a single strip spiral and strip ties, did not show any significant longitudinal bar buckling, indicating that this layout is another viable option that provides restraint to bar buckling that is comparable to that of conventional deformed reinforcing bar hoops and ties. Specimen 2SS-0.98—which violated the ACI 318-19¹ requirements for center-to-center spacing s_r , the clear spacing s_{rc} , and the volumetric confinement reinforcement ratio ρ_{st} (Table 2)—had noticeable bar buckling of the extreme middle and corner longitudinal bars. This finding indicates that maintaining the current ACI 318-19 confinement requirements for the steel strip is likely appropriate. In specimen SS-1.15, which had the single outer spiral, significant buckling was observed in both the corner and middle extreme longitudinal bars. The buckling of the corner longitudinal bars was more pronounced on the negative loading side. This finding was expected, as Barbachyn et al.⁴ had previously found that a single perimeter spiral did not sufficiently restrain longitudinal bars, particularly the middle bars, from buckling. The steel strip did not rupture in any of the specimens.

Conclusion

This paper presents a study of the measured and observed behaviors of six full-scale reinforced concrete columns subjected to reversed-cyclic lateral loading and a constant concentric axial compression load. In the investigation, the behavior of columns confined by DP, high-strength (100 ksi [690 MPa] yield strength) steel strips was compared with the behavior of a control specimen confined using deformed reinforcing bars (that is, using 100 ksi yield strength ties). The varied parameters were confinement type (strip or reinforcing

bar), confinement layout (hoops and ties, single spiral, two spirals, two out-of-phase spirals), and confinement ratio. Due to laboratory constraints, the experiments were performed at an axial load (15% of the gross section compression strength) that would be relatively low for building applications. The following conclusions refer to performance under this low axial load. Future research is warranted at greater axial loads more representative of building construction.

The major conclusions of this investigation are:

- The peak lateral strength of the strip-confined specimens was comparable to that of the reinforcing-bar-confined control specimen and exceeded the nominal lateral strength calculated based on measured material properties.
- The initial lateral stiffness of the strip-confined specimens exceeded that of the reinforcing-bar-confined control specimen, with the average stiffness of the strip-confined specimens being 55.2% greater in the positive loading direction and 19.3% greater in the negative loading direction. Because only one reinforcing-bar-confined specimen was tested, additional research is needed to further investigate any impact of strip confinement on stiffness.
- In the strip-confined specimen with out-of-phase spirals, stiffness in the two loading directions was more consistent than in the other strip-confined specimens. This finding may indicate directionality associated with the orientation of the spiral, and it may suggest that there are advantages in using two out-of-phase spirals. This is also an area for future research.
- All specimens met the ACI T1.1-01¹⁴ criteria that the lateral load at the third complete cycle for the validation drift ratio of 3.5% was not below 75% of the peak load in each direction. This finding indicates that strip confinement has the potential to provide the necessary lateral strength and ductility for reinforced concrete columns in high seismic regions.
- Relative to the reinforcing bar-confined specimen, the strip-confined specimens demonstrated improved residual lateral strength behavior. This finding indicates that the strip was able to provide a larger confined core area.
- The control specimen and the equivalent strip-confined specimen (specimen 2SS-1.32) exhibited similar axial shortening behavior, whereas the other strip-confined specimens exhibited more axial shortening. The single strip configuration showed the greatest residual axial shortening, a finding that is consistent with the larger amount of bar buckling associated with that configuration.
- In a configuration with eight longitudinal bars, an outer square strip spiral and an inner circular strip spiral is rec-

ommended, instead of a single outer square strip spiral, to better restrain longitudinal bar buckling.

- In a configuration with eight longitudinal bars, an outer square strip spiral with strip crossties and a two-strip spiral layout exhibited similar lateral load behavior and restraint from longitudinal bar buckling. However, the individual ties were more labor intensive to fabricate than the spirals, and the individual ties may result in more residual axial deformation.
- The center-to-center spacing, clear spacing, and minimum reinforcement ratio requirements of ACI 318-19 are likely appropriate for strip confinement, but additional research is necessary. The ability to develop consistent consolidation considering the geometry of the strip confinement reinforcement is an important consideration that can affect quality control and needs to be evaluated. In addition, the lateral restraint requirements of ACI 318 are likely also appropriate for strip confinement.

Overall, this research indicates that steel strip confinement is a viable strategy for earthquake-resistant design of reinforced concrete columns. Additional experimental research is necessary to investigate the impact of varying axial compression on behavior. Important directions for future research include developing validated numerical models and evaluating analytical expressions that can predict the lateral behavior of strip-confined columns for design, including a focus on lateral deformations. Furthermore, practical fabrication strategies that make it possible to rapidly uncoil the strip and form the desired geometry must be developed before this technology can be effectively deployed in real-world projects. A limit-benefit study considering material cost, fabrication time and cost, and environmental impact is necessary to fully evaluate how this technology compares to conventional reinforcing bar confinement. While this research focused on square columns for a precast concrete application, steel strip confinement offers great potential for circular cross sections, where the bending of the steel strip would also be simplified.

Acknowledgments

This paper is based on work supported by an American Concrete Institute Foundation (ACIF) Concrete Research Council grant. The authors are also grateful for support from a University of Notre Dame Recovery and Resilience Grant. The authors gratefully acknowledge the support of ACIF program directors Ann Masek and Tricia Ladely, and ACI Committee 550 representatives Suzanne Aultman and Larbi Sennour. The support and guidance from the Industry Advisory Group is also acknowledged. That group includes Don Meinheit (independent consultant), Clay Putnam (Metromont Corp.), Mark Sarkisian and Austin Devin (Skidmore, Owings & Merrill), Ted Zoli (HNTB Corp.), Adam Reihl (StresCore Inc.), Matt Ballain (Coreslab Structures Inc.), Nathan Krause and Bruce Hopkins (Fabcon), and Jared Brewe (PCI). The authors gratefully acknowledge ArcelorMittal for its generous

donation of steel product. Without this donation, the work would not have been possible. Any findings, conclusions, or recommendations in this report are those of the authors and do not necessarily represent the views of the organizations/individuals acknowledged.

References

1. ACI (American Concrete Institute). 2019. *Building Code Requirements for Structural Concrete (ACI 318-19) and Commentary (ACI 318R-19)*. Farmington Hills, MI: ACI.
2. ASTM International. 2022. *Standard Specification for Deformed and Plain Carbon-Steel Bars for Concrete Reinforcement*. ASTM A615/A615M-22. West Conshohocken, PA: ASTM International.
3. ASTM International. 2024. *Standard Specification for Deformed and Plain, Low-Carbon, Chromium, Steel Bars for Concrete Reinforcement*. ASTM A1035/A1035M-24. West Conshohocken, PA: ASTM International.
4. Barbachyn, S. B., A. O'Donnell, A. P. Thrall, and Y. C. Kurama. 2023. "Axial Load Behavior of Reinforced Concrete Columns with High-Strength Steel Coiled Strips as Confinement." *PCI Journal* 68 (5): 21–41. <https://doi.org/10.15554/pcij68.5-01>.
5. Kidder, F. E., and T. Nolan. 1911. *Building Construction and Superintendence*. New York, NY: William T. Comstock.
6. Shafqat, A., and A. Ali. 2012. "Lateral Confinement of RC Short Column." *Science International (Lahore)* 24 (4): 371–379.
7. Tahir, M. F., Q. U. Z. Khan, and A. Ahmad. 2015. "Effect of Concrete Strength on Behavior of Strip Confined Columns." *Technical Journal, University of Engineering and Technology Taxila* 19 (2): 28–34. <https://tj.uettaxila.edu.pk/older-issues/2014/No2/Chapter-5.pdf>.
8. Rizwan, M. 2009. "Performance of RC Structures under Earthquake Loading." PhD diss. University of Engineering and Technology, Lahore, Pakistan.
9. Rizwan, M., S. A. Khan, M. Ilyas, and R. R. Hussain. 2016. "Modelling Steel-Strip-Confined Reinforced-Concrete Columns." *Structures and Buildings* 169 (4): 245–256. <https://doi.org/10.1680/jstbu.14.00084>.
10. ASTM International. 2021. *Standard Test Method for Compressive Strength of Cylindrical Concrete Specimens*. ASTM C39/C39M-21. West Conshohocken, PA: ASTM International.
11. ASTM International. 2022. *Standard Test Method for Static Modulus of Elasticity and Poisson's Ratio of*

Concrete in Compression. ASTM C469/C469M-22. West Conshohocken, PA: ASTM International.

12. ASTM International. 2022. *Standard Test Methods and Definitions for Mechanical Testing of Steel Products*. ASTM A370-22. West Conshohocken, PA: ASTM International.

13. ASTM International. 2017. *Standard Test Method for Young's Modulus, Tangent Modulus, and Chord Modulus*. ASTM E111-17. West Conshohocken, PA: ASTM International.

14. ACI. 2001. *Acceptance Criteria for Moment Frames Based on Structural Testing*. T1.1-01. Farmington Hills, MI: ACI.

Notation

A_{ch} = cross-sectional area of concrete core measured to the outside edges of the confinement reinforcement

A_g = gross cross-sectional concrete area

d_b = reinforcing bar diameter

E_c = measured concrete elastic modulus

E_n = nominal lateral resistance calculated using specified material properties

E_{pr} = nominal lateral resistance calculated based on measured material properties

E_s = measured steel elastic modulus

f'_c = measured concrete compressive strength

f'_{dc} = design concrete compressive strength

f_{sy} = specified steel yield strength

f_{syl} = specified longitudinal steel yield strength

f_{syt} = specified confinement steel yield strength

f_u = measured steel peak strength

f_y = measured steel yield strength

f_{yl} = measured longitudinal steel yield strength

f_{yt} = measured confinement steel yield strength

h_w = specimen height

K_i = initial stiffness

n_b = number of longitudinal bars

s_t = center-to-center spacing of confinement steel

$s_{t,max}$ = maximum permitted center-to-center spacing of confinement steel

s_{tc} = clear spacing of confinement steel

$s_{tc,min}$ = minimum required clear spacing of confinement steel

$s_{tc,max}$ = maximum permitted clear spacing of confinement steel

t_s = steel strip thickness

V_c = lateral load at initial column cracking

V_p = peak lateral load

V_v = lateral load at validation-level drift

w_s = steel strip width

Δ = drift

Δ_p = drift at peak lateral load

ϵ_r = measured steel strain at rupture

ϵ_u = measured steel strain at peak strength

ϵ_y = measured steel strain at yield

ρ_{st} = longitudinal steel reinforcement ratio

ρ_{st} = volumetric reinforcement ratio of confinement steel

$\rho_{st,min1}$ = minimum volumetric reinforcement ratio of confinement steel per Eq. (1)

$\rho_{st,min2}$ = minimum volumetric reinforcement ratio of confinement steel per Eq. (2)



Steven M. Barbachyn, PhD, is a research associate and the manager of the Galambos and MAST Structural Engineering Laboratories at the University of Minnesota in Minneapolis. This research was performed when he was a postdoctoral research associate in the Department of Civil and Environmental Engineering and Earth Sciences at the University of Notre Dame in Notre Dame, Ind.



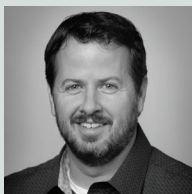
Shane Oh was a graduate student at the University of Notre Dame when this research was performed.



Lily A. Pearson is a project engineer at Frost Engineering and Consulting. At the time this research was performed, she was a graduate student at the University of Notre Dame.



Ashley Thrall, PhD, is the Myron and Rosemary Noble Associate Professor of Structural Engineering in the Department of Civil and Environmental Engineering and Earth Sciences at the University of Notre Dame.



Brad Weldon, PhD, is the Henry Massman Teaching Professor of Civil Engineering at the University of Notre Dame.



Yahya Kurama, PhD, PE, is a professor in the Department of Civil and Environmental Engineering and Earth Sciences at the University of Notre Dame.

Abstract

This paper presents the experimental investigation of the behavior of square reinforced concrete columns

with high-strength (100 ksi [690 MPa]) steel coiled strips as embedded confinement reinforcement under reversed-cyclic lateral loading and constant axial compression load. Six full-scale specimens (20 × 20 in. [508 × 508 mm] cross section) with the following variations were tested: confinement type (strip or reinforcing bar), layout (hoops and ties, spirals), and reinforcement ratios. The strip-confined specimens had similar peak strengths as a specimen confined by reinforcing bar ties, and this strength exceeded analytical predictions. The stiffness of the strip-confined specimens was greater than the reinforcing-bar-confined specimen. In accordance with the American Concrete Institute's *Acceptance Criteria for Moment Frames Based on Structural Testing* (T1.1-01), all specimens met the criterion that the lateral load at 3.5% drift was not below 75% of the peak. Strip-confined specimens demonstrated improved residual strength behavior relative to the reinforcing-bar-confined specimen. Overall, the study demonstrated the promise of steel strip confinement for reinforced concrete columns in seismic regions.

Keywords

Column, confinement, high-strength steel, lateral load, reinforced concrete, strip reinforcement.

Review policy

This paper was reviewed in accordance with the Precast/Prestressed Concrete Institute's peer-review process. The Precast/Prestressed Concrete Institute is not responsible for statements made by authors of papers in *PCI Journal*. No payment is offered.

Publishing details

This paper appears in *PCI Journal* (ISSN 0887-9672) V. 70, No. 1, January–February 2025, and can be found at <http://doi.org/10.15554/pcij70.1-01>. *PCI Journal* is published bimonthly by the Precast/Prestressed Concrete Institute, 8770 W. Bryn Mawr Ave., Suite 1150, Chicago, IL 60631. Copyright © 2025, Precast/Prestressed Concrete Institute.

Reader comments

Please address any reader comments to *PCI Journal* editor-in-chief Tom Klemens at tklemens@pci.org or Precast/Prestressed Concrete Institute, c/o *PCI Journal*, 8770 W. Bryn Mawr Ave., Suite 1150, Chicago, IL 60631. 